Supplementary Information
for

Template-Assisted Synthesis of Multi-Shelled Carbon Hollow Spheres with Ultralarge Pore Volume as Anode Materials in Li-Ion Batteries

Zhuang Sun,[a,b] Xuefeng Song,*[a,b] Peng Zhang[a,b] and Lian Gao*[a,b]

State Key Laboratory for Metallic Matrix Composite Materials,

School of Materials Science and Engineering,

Shanghai Jiao Tong University, Shanghai, 200240, China.

*E-mail address: liangao@mail.sic.ac.cn (L. Gao); songxfeng@sjtu.edu.cn (X. Song)

Tel: +86-12-52412718. Fax: +86-21-52413122

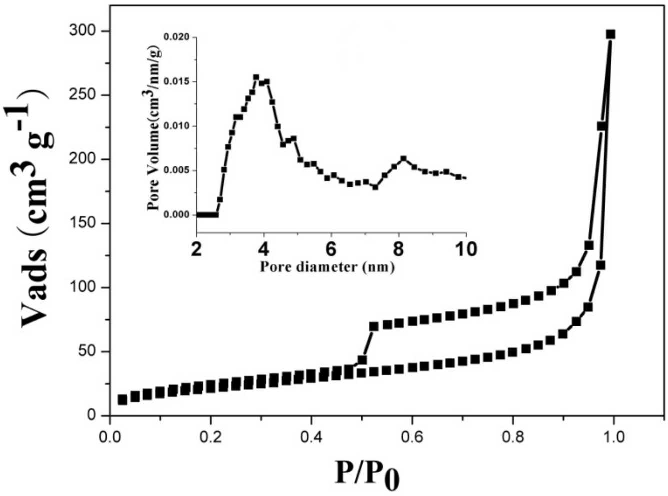

Figure S1 The nitrogen adsorption-desorption isotherm with corresponding pore size distributions (inset) of MSHS.

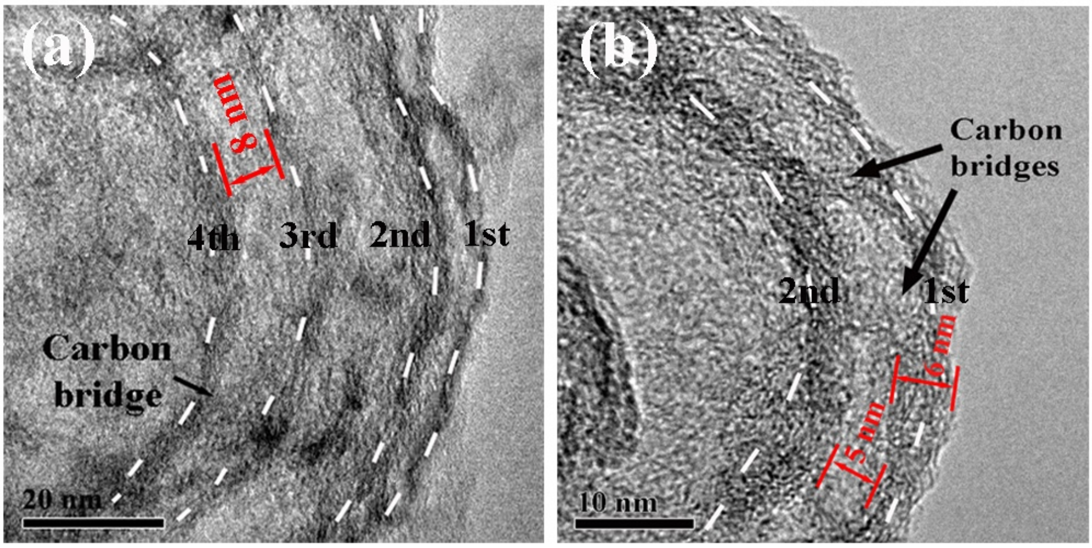

Figure S2 The HRTEM images of (a) QCHS and (b) DCHS.

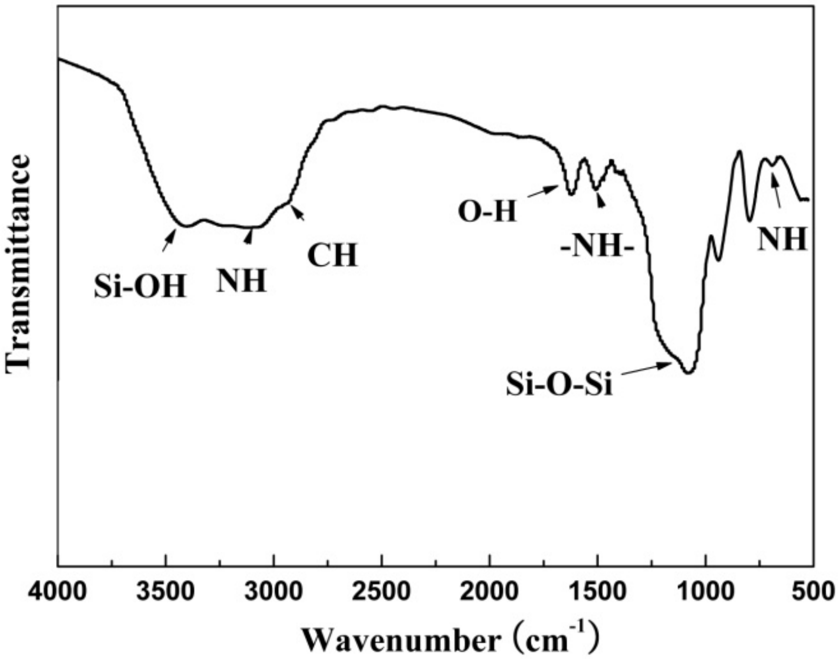

Figure S3 FTIR spectrum of amino-functionalized silica hollow spheres.

The synthesis of SCHS:

Single-shelled carbon hollow spheres (SCHS) were generated by using amino-functionalized solid silica spheres as templates, which were synthesized following the Stober method[1] and amino-functional step (the as-prepared solid silica spheres (0.15 g) were mixed with APTES (0.025 mol) in 2.4 ml methanol and stirred for 4 hr, washed by ethanol at least 4 times and dried in air at 60 °C). Monodispersed silica sphere with an average diameter of about 120 nm can be observed in Figure S5a, and were coated with a glucose-derived polysaccharide on the surface of the silica template. After HF etching, single-shelled carbon hollow spheres were generated with an average diameter of 120 nm (Figure. S5b).

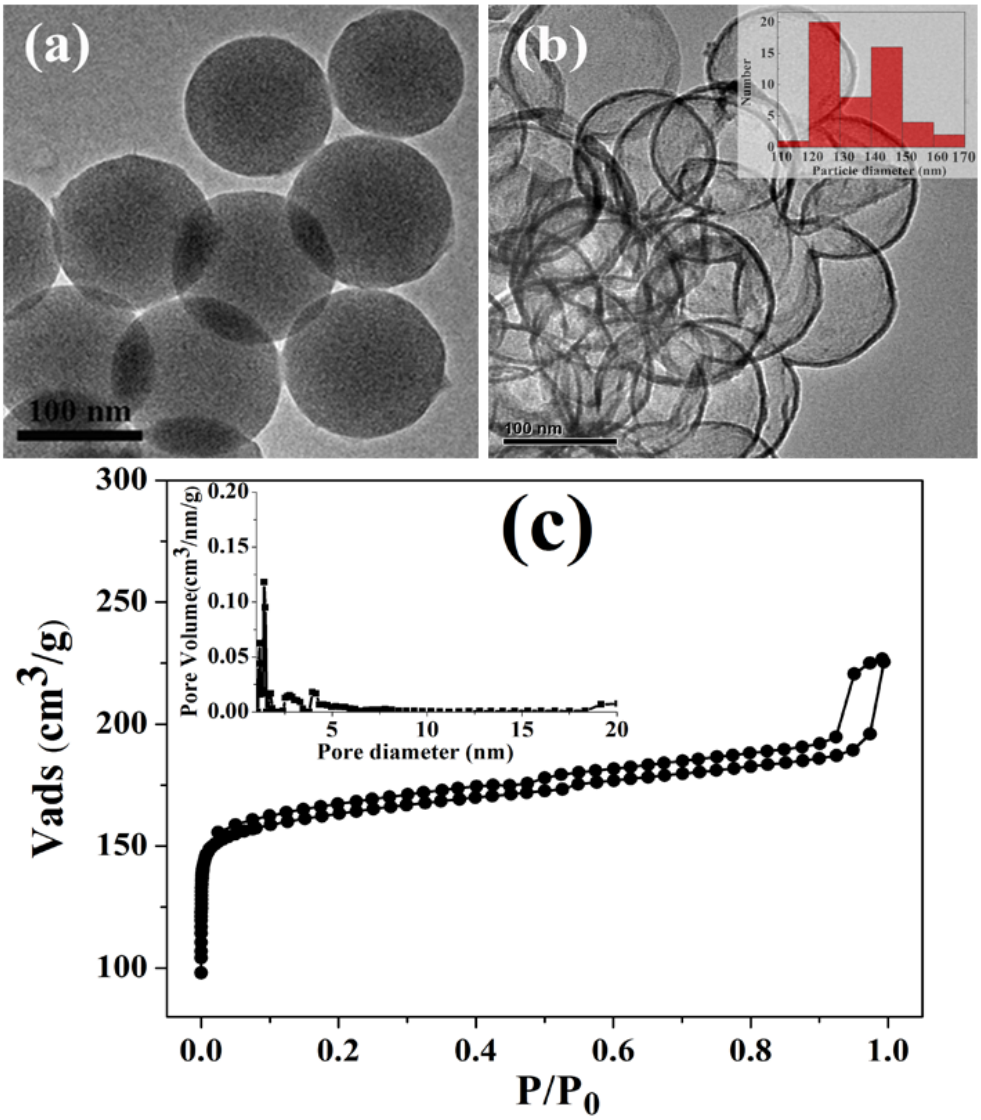

Figure S4 The TEM images of (a) silica spheres and (b) SCHS. (c) The nitrogen adsorption-desorption isotherm with corresponding pore size distributions (inset) of SCHS.

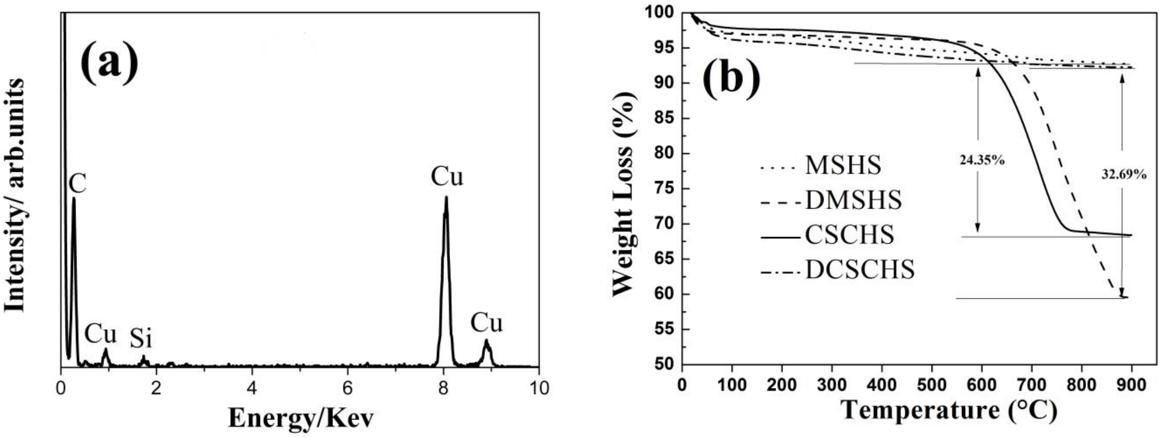

Figure S5 (a) The EDS analyses of the prepared QCHS. (b) The TG curves of the pristine silica templates (MSHS and DMSHS) and intermediates (CSCHS and DCSCHS).

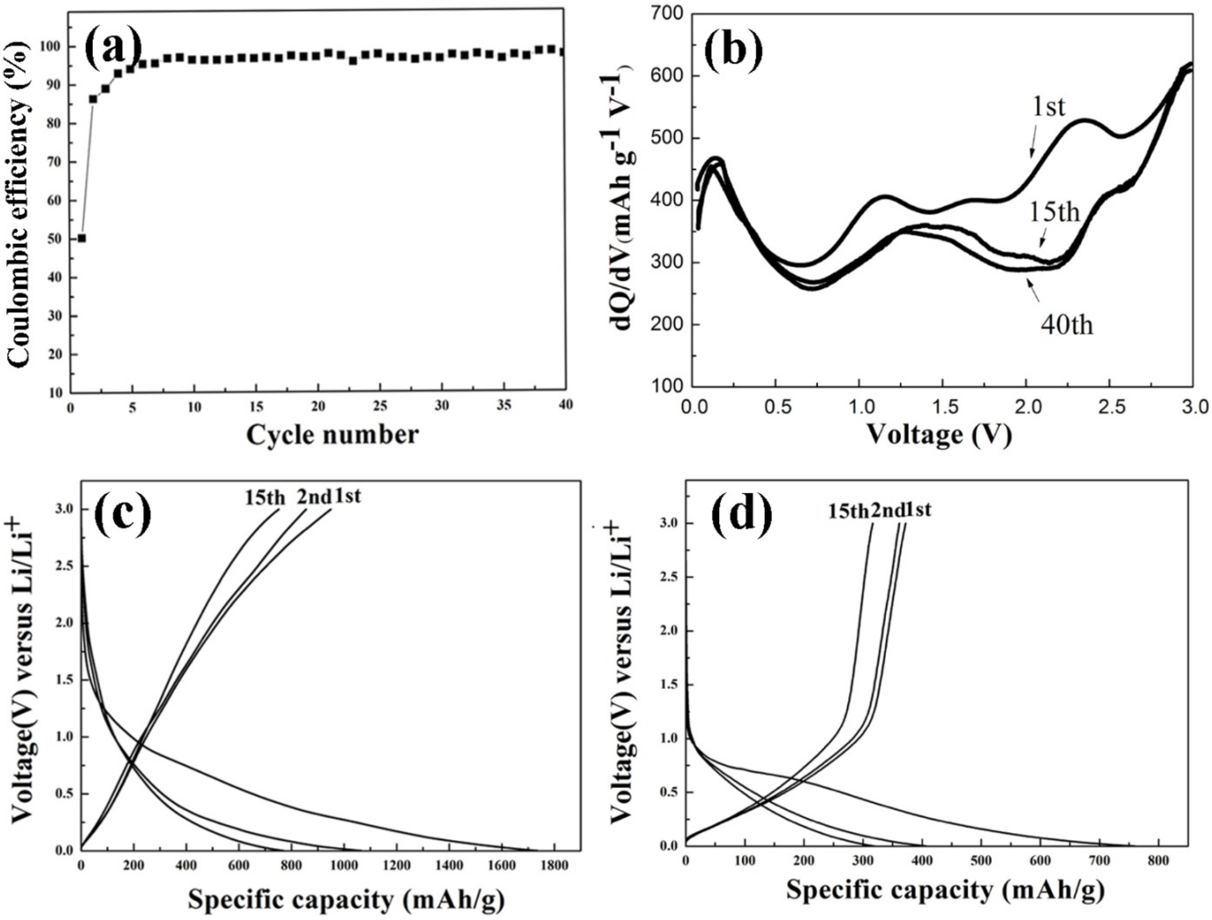

Figure S6 (a) Coulombic efficiency of the QCHS during 40 cycles. (b) Differential capacity versus cell voltage plots of QCHS during charging process. Galvanostatic charge/discharge curves of (c) DCHS and (d) SCHS at a current rate of 50 mA g^{-1}.

Approximate calculation on the volume occupying rate for the multi-shelled hollow spheres:

The volume occupying rate of multi-shelled hollow sphere is significant to evaluate the void-space utilizing rate, which is essential to get high lithium storage capacity.[14] From the TEM image (Figure S8), the diameter and the thickness of an SCHS are ~120 nm and ~6 nm, respectively. So the volumes of the total hollow sphere, the void space in the core and the carbon shell are 9.04×10^{-4} um^3, 6.59×10^{-4} um^3, and 2.45×10^{-4} um^3, respectively. Accordingly, the volume occupy of active material is about 27% of the total space for the SCHS. Similarly, the volume occupying rates of the total space are calculated to be 47% for DCHS and 55% for QCHS, according to the formulas bellow:

Equation S1:

Volume occupying rate (SCHS) = $V_{shell}/V_1=(V_1-V_2)/V_1=27$ % ($r_1=60$ nm, $r_2=54$ nm, the shell thickness: ~6 nm)

Equation S2:

Volume occupying rate (DCHS) = $V_{shell}/V_1=[(V_1-V_2)+(V_3-V_4)]/V_1=47$ % ($r_1=55$ nm, $r_2=49$ nm, $r_3=44$ nm, $r_4=38$ nm, the shell thickness:~6 nm)

Equation S3:

Volume occupying rate (QCHS) = $V_{shell}/V_1= [(V_1-V_2)+(V_3-V_4)+(V_5-V_6)+(V_7-V_8)] /V_1 =55$ % ($r_1=74$ nm, $r_2=68$ nm, $r_3=65$ nm, $r_4 =59$ nm, $r_5=53$ nm, $r_6=47$ nm, $r_7=42$ nm, $r_8=36$ nm, the shell thickness:~6 nm)

Where V_1 is the volume of the total hollow sphere, V_{shell} is the volume of the carbon shell, V_2~V_8 are the volumes of the void spaces in the cores (as shown in the Figure S8).

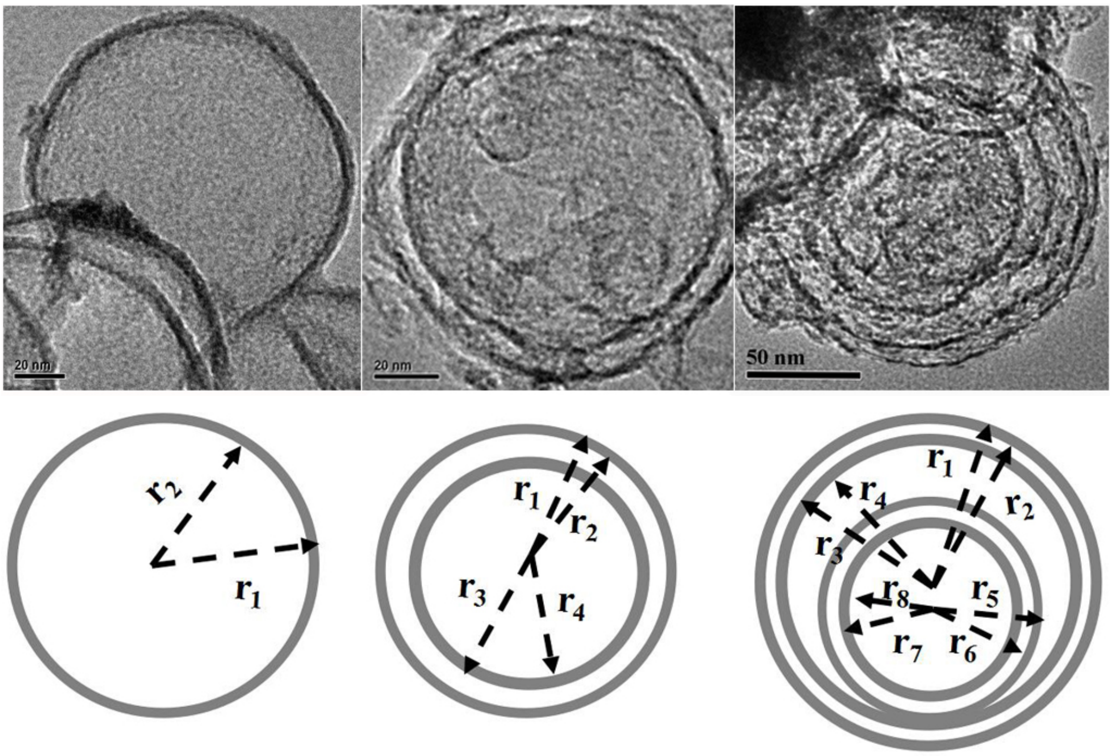

Figure S7 Simple modeling of SCHS, DCHS and QCHS.

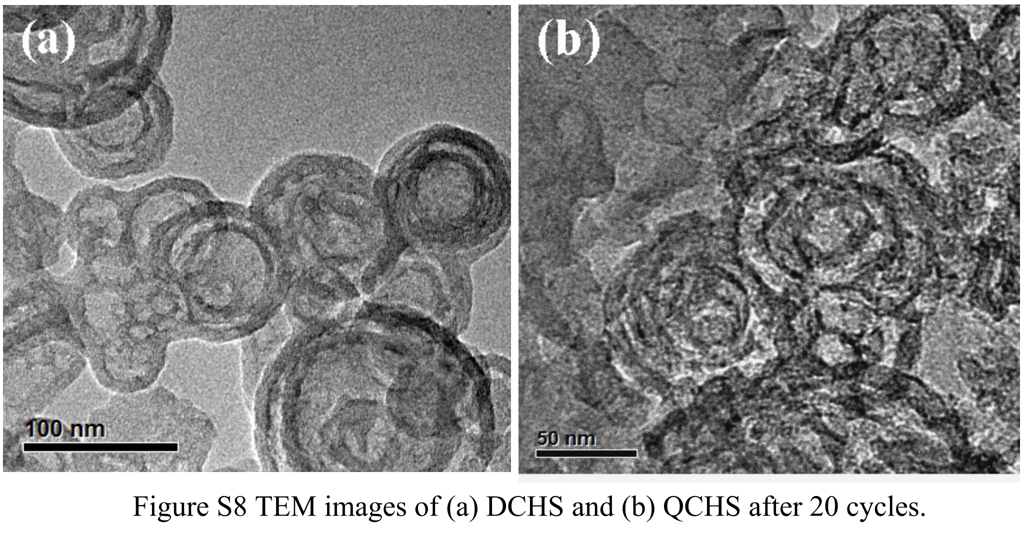

Figure S8 TEM images of (a) DCHS and (b) QCHS after 20 cycles.

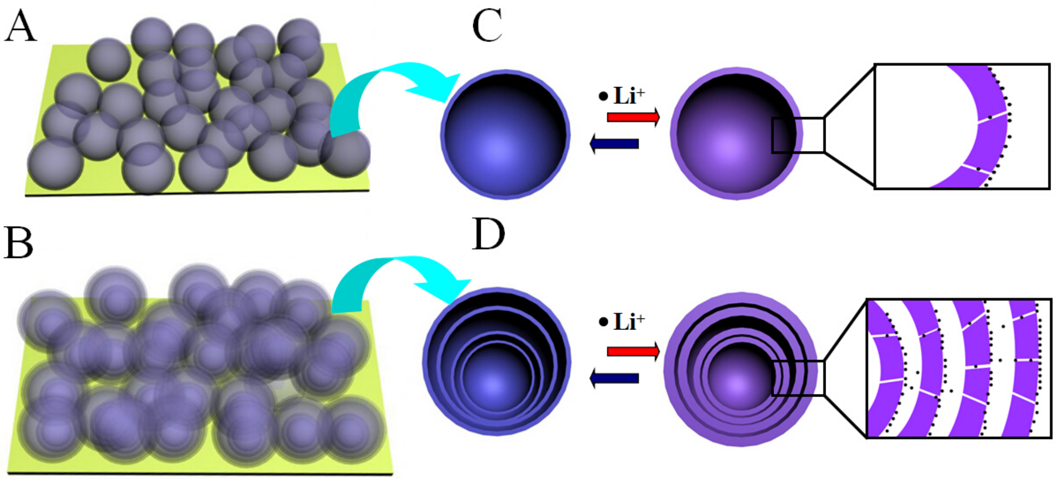

Scheme S1. Schematic of the materials design. (a) A conventional slurry coated SCHS electrode. (b) A novel QCHS electrode. Magnified schematics of an individual SCHS (c) and QCHS (d) particles showing that the QCHS have larger active surface area per unit volume than SCHS.

Table S1. Surface area/pore volume and specific capacity values of analogous anode materials

Materials	BET surface area (m^2 g^{-1})/ Pore volume (cm^3 g^{-1})	Specific capacity (mAh g^{-1})	Ref
QCHS	1533/3.02	978 after 40 cycles at 50 mA g^{-1}	This work
DCHS	1064/1.89	712 after 40 cycles at 50 mA g^{-1}	This work
SCHS	644/0.29	304 after 40 cycles at 50 mA g^{-1}	This work
Nanographene-constructed hollow carbon spheres	970/-	600 after 30 cycles at a rate of C/5	Ref [2]
Double shelled hollow carbon/sulfur spheres	748/1.685	690 after 100 cycles at 167.5 mA g^{-1} for Li-sulfur cathode	Ref [3]
Interconnected hollow carbon nanospheres	412/-	310 after 200 cycles at a rate of 1C	Ref [4]
The spherical hollow carbon nanospheres	466/1.6 for MPG-C130nm-550°C	-	Ref [5]
Hollow carbon nanotube/ carbon nanofiber hybrid	1840/1.21	1150 after 70 cycles at 0.1 A g^{-1}	Ref [6]
Tube-in-tube structured carbon nanomaterials (As the host for sulfur cathode)	882.8/1.77	918 (based on sulfur) or 652 (based on S-TTCN composite) after 50 cycles.	Ref [7]
Crumpled nitrogen-doped graphene nonosheets	465.0/3.42 carbonized at 900°C	-	Ref [8]
Hierarchically porous carbon monoliths	327/0.59 carbonized at 850°C	500 after 15 cycles at a rate of C/5	Ref [9]
Highly-ordered mesoporous carbon nitride nanorods	971−1124/ 1.31-1.79	-	Ref [10]
Porous carbon nanospheres (PCNS) Active- carbon PCNS (a-PCNS) Tailored-pore PCNS (p-PCNS) (As the host for sulfur cathode)	550/3.3 for PCNS 1800/5.4 for a-PCNS 763/2.65 for p-PCNS-L 956/3.42for p-PCNS-M 1055/2.41 for p-PCNS-H	700 after 100 cycles at 1675 mA g^{-1} (a-PCNS) 725 after 100 cycles at 625 mA g^{-1} (p-PCNS-M)	Ref [11]

High pore volume carbon	1800/6.0	-	Ref [12]
Peapodlike mesoporous carbon (As the host for sulfur cathode)	977/4.69	300~400 after 50 cycles (based on the mass of the C/S composites)	Ref [13]

References

1 W. StÖber and A. Fink, *J. Colloid Interf. Sci.*, 1968, **26**, 62.

2 S. B. Yang, X. L. Feng, L. J. Zhi, Q. Cao, J. Maier and K. Müllen, *Adv. Mater.*, 2010*,* **22***,* 838.

3 C. F. Zhang, H. B. Wu, C. Z. Yuan, Z. P. Guo and X. W. Lou, *Angew. Chem. Int. Ed.*, 2012, **51**, 9592.

4 K. Tang, R. J. White, X. K. Mu, M. M. Titirici, P. A. van Aken and J. Maier, *ChemSusChem*, 2012, **5**, 400.

5 R. J. White, K. Tauer, M. Antonietti and M. Titirici, *J. Am. Chem. Soc.*, 2010, **132**, 17360.

6 Y. M. Chen, X. Y. Li, K. Park, J. Song, J. H. Hong, L. M. Zhou, Y. W. Mai, H. T. Huang and J. B. Goodenough, *J. Am. Chem. Soc.*, 2013, **135**, 16280.

7 Y. Zhao, W. L. Wu, J. X. Li, Z. C. Xu and L. H. Guan, *Adv. Mater.*, DOI 10.1002/adma. 201401191.

8 Z. H. Wen, X. C. Wang, S. Mao, Z. Bo, H. Kim, S. M. Cui, G. H. Lu, X. L. Feng and J. H. Chen, *Adv. Mater.*, 2012, **24**, 5610.

9 Y. S. Hu, P. Adelhelm, B. M. Smarsly, S. Hore, M. Antonietti and J. Maier, *Adv. Funct. Mater.*, 2007, **17**, 1873.

10 Z. K. Zhao, Y. T. Dai, J. H. Lin and G. R. Wang, *Chem. Mater.*, 2014, **26***,* 3151.

11 G. He, S. Evers, X. Liang, M. Cuisinier, A. Garsuch and L. F. Nazar, *ACS Nano*, 2013, **7**, 10920.

12 K. P. Gierszal and M. Jaroniec, *J. Am. Chem. Soc.*, 2006, **128**, 10026.

13 D. Li, F. Han, S. Wang, F. Cheng, Q. Sun and W. C. Li, *ACS Appl. Mater. Interfaces*, 2013, **5**, 2208.

14 X. Wang, X. L. Wu, Y. G. Guo, Y. T. Zhong, X. Q. Cao, Y. Ma and J. N. Yao, *Adv. Funct. Mater.*, 2010, **20**, 1680.